eng

MDPI

Article

Assessment of Analytical Methods for Estimating Settlements Induced by Side-by-Side Twin Tunnels

António M. G. Pedro [1,*], José C. D. Grazina [2] and Jorge Almeida e Sousa [3]

[1] Institute for Sustainability and Innovation in Structural Engineering (ISISE), Advanced Production and Intelligent Systems (ARISE), Department of Civil Engineering, University of Coimbra, 3030-788 Coimbra, Portugal
[2] Infraestruturas de Portugal, 1750-130 Lisboa, Portugal; jose.grazina.ext@infraestruturasdeportugal.pt
[3] Department of Civil Engineering, University of Coimbra, 3030-788 Coimbra, Portugal; jas@dec.uc.pt
* Correspondence: amgpedro@dec.uc.pt; Tel.: +351-23-979-7224

Abstract: The development of urban areas has led to an increase in the use of subsoil for installing transportation networks. These systems usually comprise the construction of side-by-side twin running tunnels built sequentially and in close proximity. Different studies have demonstrated that under such conditions, there is an interaction between tunnels, leading to greater settlements compared with those obtained if the tunnels were excavated separately. Supported by those findings, several analytical methods have been proposed to predict the settlements induced by the excavation of the second tunnel. This paper examines the applicability of these proposals across multiple case studies published in the literature by comparing the analytical predictions with the reported monitoring data of 57 sections. The results indicate that, regardless of the different soil conditions and geometrical characteristics of the tunnels, a Gaussian curve accurately describes the settlements in greenfield conditions and those induced by the second tunnel excavation, although with the curve becoming eccentric in this case. Despite some significant scatter observed, most methods predict the settlements induced by the second tunnel with reasonable accuracy, with Hunt's method presenting the best fit metrics. The obtained findings confirm that existent methods can be a valid tool to predict the settlements induced by twin tunnelling during the early stages of design, although do also contain limitations and pitfalls that are identified and discussed throughout the paper.

Keywords: twin tunnelling; analytical methods; monitoring data

Received: 16 December 2024
Revised: 15 January 2025
Accepted: 23 January 2025
Published: 26 January 2025

Citation: Pedro, A.M.G.; Grazina, J.C.D.; Almeida e Sousa, J. Assessment of Analytical Methods for Estimating Settlements Induced by Side-by-Side Twin Tunnels. *Eng* **2025**, *6*, 25. https://doi.org/10.3390/eng6020025

1. Introduction

In densely populated urban centres, efficient and sustainable transportation networks are vital for economic development [1]. Factors such as the limited space at the ground surface, traffic congestion, and growing demands for sustainability and cleaner environments have driven the construction and relocation of transportation networks into the subsoil [2]. Despite the complexity associated with the construction, these underground networks provide higher mobility and are more reliable and efficient than surface solutions, making them a cost-effective asset for any city [3]. Solutions such as side-by-side twin tunnels, in opposition to the construction of a single larger tunnel, are often preferred for these infrastructures since traffic can flow separately in opposite directions, thus minimizing the congestion and number of collisions while maximizing the speed and safety of travelling. The excavation process itself is often simpler in this case, as the

construction of smaller tunnels is quicker, requires less support, and can be performed at shallower depths, reducing the costs without compromising the stability and safety of the excavations.

However, regardless of the construction method employed, the excavation of tunnels will inevitably induce movements in the surrounding soil, which, in shallower tunnels, extend to the ground surface and affect the structures located in the vicinity of the excavation [4]. Naturally, the magnitude and extent of these ground movements are influenced by several factors, such as the tunnel geometry, the soil and groundwater conditions, and the excavation method employed [5]. In order to perform an adequate risk assessment of the structures during the preliminary design stage, a quick yet reliable estimation of the magnitude and extent of the ground movements induced by the tunnel excavations is required [6,7]. For a single tunnel excavation, the typical settlement profile is well documented in the literature and, amid other proposals [8], can be reasonably approximated as an inverted Gaussian distribution curve, as suggested by Peck [9]. However, the case of side-by-side twin tunnels is more complex, with several studies (see Table 1) showing that the excavation of the second tunnel (2T) induces higher settlements when compared with those caused by the construction of the first tunnel (1T). Moreover, it has been observed that the final settlement trough shows some asymmetry, with the maximum settlement occurring closer to the 1T, rather than being centred between the tunnels [10–12]. According to Mair and Taylor [7], this interaction effect occurs as the 2T is excavated in disturbed ground conditions and is fundamentally dependent on the distance between tunnels, usually referred to as pillar width (P). However, recent advances in EPB (earth pressure-balanced shield) technology have made it possible to adjust shield operational parameters, such as the face or grouting pressure, so that the settlements induced by the 2T excavation can be compensated and reduced significantly, as the results of Suwansawat and Einstein [13] have demonstrated.

The interaction between side-by-side twin tunnels has been widely documented in various case studies (see Table 1), but has also been investigated through numerical [14–24], centrifuge [4], and small-scale models [25–28]. An extensive compilation and review of those studies has already been presented and summarized by Vlachopoulos et al. [29] and, more recently, by Islam and Iskander [5]. These studies assess aspects such as the lining forces interaction [30,31], the overall tunnel stability [32,33], and the stress redistribution along the pilar width [34,35], but are primarily focused on evaluating the ground movements and volume loss induced by the excavation of the 2T and on assessing the distance between tunnels at which interaction effects can be considered negligible. Based on the results provided by these studies, several analytical methods have been proposed to quantify the settlements and sub-surface vertical displacements caused by side-by-side twin tunnel excavation [4,16,22,36–40]. Despite the differences among them, all proposals assume that the settlement profile induced by the excavation of the 1T is described by an inverted Gauss distribution curve and then use those Gaussian fitting parameters, along with the distance between the tunnels, to predict the additional volume loss induced by the 2T excavation. Although these analytical methods are of simple application and can provide valuable insights during the preliminary design stage, they were developed for specific cases, and their applicability to real case studies has yet to be fully validated. This paper discusses the applicability of those analytical methods by comparing their prediction against the monitoring data reported for a vast number of case studies published in the literature. The aim of this paper is to highlight the strengths and limitations of each of these analytical methods, enabling more informed decision-making when predicting settlements induced by twin tunnelling.

Table 1. List of the case studies analyzed.

Source	Project	Excavation Method	Ground Conditions	Section	Code	D (m)	Z_0 (m)	d (m)	P (m)
Cording and Hansmire [10]	Washington D. C. Metro	Shield machine	Granular soil	C	A	6.40	14.60	11.00	4.60
Perez Saiz et al. [11]	Caracas Metro	EPB	Soft rock	S-IV	B	5.60	11.20	12.00	6.40
Ou et al. [41]	Taipei RTR	EPB	Fine soil	CH218 A-A	C	6.04	16.00	18.00	11.96
Withers [42]	London Metro, Jubilee Line	EPB	Soft rock	Old Jamaica R.	D1	4.90	19.50	26.00	21.10
				Southwark P.	D2	4.90	20.80	27.50	22.60
Wu and Lee [43]	Taipei RTR	EPB	Fine soil	CN254 S2	E1	6.04	14.30	13.20	7.16
	Japan Subway	Open shield	Fine soil	B-1	E2	7.06	27.50	10.00	2.94
Clayton et al. [44]	Heathrow E. T4	Sequential	Stiff clay	MMS II	F	9.00	17.90	27.00	18.00
Suwansawat and Einstein [13]	Bangkok MRTA	EPB	Stiff clay	S-A 23-AR-001	G1	6.50	22.00	10.50	4.00
				S-B 26-AR-001	G2	6.50	18.50	20.00	13.50
				S-C CS-8B	G3	6.50	19.00	18.00	11.50
				S-C CS-8D	G4	6.50	20.10	14.50	8.00
				S-D SS-5T-52e	G5	6.50	22.20	20.00	13.50
Mahmutoğlu [45]	Istanbul Subway	EPB	Granular soil	S-3a	H1	6.50	17.00	15.00	8.50
				S-3b	H2	6.50	17.00	15.00	8.50
Bilotta and Russo [46]	Naples Metro	EPB	Granular soil	S-1	I1	6.74	17.00	13.80	7.06
				S-2	I2	6.74	17.00	15.00	8.26
				S-3	I3	6.74	17.00	15.40	8.66
He et al. [27]	Chengdu Metro	EPB	Granular soil	-	J	6.00	11.00	8.00	2.00
Standing and Selemetas [47]	Channel Tunnel Rail Link	EPB	Stiff clay	C250	K	8.16	19.50	16.00	7.84
Ocak [37]	Istanbul Subway	EPB	Fine soil	S-4	L1	6.50	35.85	14.00	7.50
				S-5	L2	6.50	17.32	14.80	8.30
				S-8	L3	6.50	20.93	14.80	8.30
Fargnoli et al. [12]l	Milan Metro	EPB	Granular soil	S-2	M1	6.70	15.00	15.00	8.30
				S-5	M2	6.70	15.00	15.00	8.30
				S-13	M3	6.70	15.00	15.00	8.30
				S-16	M4	6.70	15.00	15.00	8.30
				S-19	M5	6.70	15.00	15.00	8.30
				S-35	M6	6.70	15.00	16.70	10.00
Elwood and Martin [48]	Edmonton Light Rail	Sequential	Soft rock	S-C	N1	6.50	13.25	11.50	5.00
				S-E	N2	6.50	13.75	8.00	1.50
Wan et al. [49]	Crossrail	EPB	Stiff clay	x-line	O1	7.10	34.50	16.30	9.20
				y-line	O2	7.10	34.50	16.30	9.20
				Extensometer	O3	7.10	34.50	16.30	9.20
Zhong et al. [50]	Chongqing Metro	EPB	Soft rock	Fengzhong R.	P	6.25	8.73	11.00	4.75
Zhou et al. [38]	Changsha Metro	EPB	Soft rock	-	Q	6.00	23.30	13.50	7.50
Kannangara et al. [51]	Hangzhou Metro	EPB	Fine soil	DBC7	R1	6.20	10.60	15.60	9.40
				DBC9	R2	6.20	10.90	15.60	9.40
				DBC11	R3	6.20	12.60	17.00	10.80
				DBC13	R4	6.20	13.90	24.10	17.90
				DBC15	R5	6.20	14.38	36.00	29.80
				DBC35	R6	6.20	15.36	15.60	9.40
				DBC36	R7	6.20	14.63	15.60	9.40
Dong et al. [40]	Changsha Metro	EPB	Soft rock	Case 1	S1	6.00	18.00	13.00	7.00
	Shenyang Utility	EPB	Granular soil	Case 2	S2	6.00	18.00	12.00	6.00
Hu et al. [52]	Tianjin Metro	EPB	Fine soil	S-A-A	T	8.80	20.60	15.80	7.00

2. Materials and Methods

2.1. Analytical Methods for Predicting Ground Movements Induced by Twin Tunnelling

The first attempt to predict the settlements induced by side-by-side twin tunnelling was proposed by O'Reilly and New [36], consisting of the superposition of two identical

Gauss curves, each one aligned with the centerline of each tunnel, with the final settlement given as expressed by Equation (1):

$$\delta_v(x) = \delta_{v,max} \cdot \left[e^{\left(-\frac{x^2}{2 \cdot i^2}\right)} + e^{\left(-\frac{(x-d)^2}{2 \cdot i^2}\right)} \right] \quad (1)$$

where d represents the distance between the centrelines of the tunnels, x is the horizontal distance measured from the centerline of 1T (note that 1T is assumed as being located on the left hand side), and $\delta_{v,max}$ and i are the Gauss parameters, with $\delta_{v,max}$ corresponding to the maximum settlement estimated at the tunnel centerline and i to the trough width parameter, which represents the distance from the centerline to the inflexion point of the Gauss curve. In the absence of field data, the estimation of the Gauss parameters is usually performed using correlations established in the literature. The trough width parameter is usually correlated with the depth of the axis of the tunnel (Z_0) by Equation (2):

$$i = K \cdot Z_0 \quad (2)$$

where K is the dimensionless trough width factor, whose value is associated with the soil characteristics [7,36]. According to Mair and Taylor [7], K typically ranges between 0.4 and 0.6 in clays and 0.25 and 0.45 for granular materials, with the average values of these intervals often being taken as representative values. In stratified soils, as is often the case, the diverse nature of the materials causes the K value to vary more broadly, making it more difficult to establish a representative value or interval. The value of $\delta_{v,max}$ is typically determined using Equation (3), using the estimated volume loss, V_s (expressed as a percentage of tunnel face volume per unit length of tunnel), as reference.

$$\delta_{v,max} = \sqrt{\frac{\pi}{32}} \cdot \frac{V_s \cdot D^2}{i} \quad (3)$$

where D is the tunnel diameter. V_s depends on the tunnel characteristics, soil conditions, and excavation method, with reported values varying between 0.1 and 3.3% [5]. Naturally, with the recent advances in technology, it is possible to reduce V_s to almost zero if adequate shield operational parameters are employed when excavating with a EPB machine [53].

The equation proposed by O'Reilly and New [36] assumes that both tunnels induce the same V_s, implicitly disregarding any interaction between them. As a result, this proposal is only acceptable when the tunnels are reasonably spaced apart (a pillar to diameter (P/D) ratio greater than 4) or when the tunnels are driven almost simultaneously [54]. While still used as reference, several studies have shown that the O'Reilly and New [36] proposal is not adequate for estimating settlements induced by side-by-side twin tunnels, as interaction effects between the tunnels are not considered.

To assess the interaction between side-by-side tunnels, Addenbrooke and Potts [16] conducted a series of coupled consolidation 2D numerical analyses, where the distance between tunnel centerlines (d) varied from 8 to 32 m (P/D between 1.0 and 7.0). Based on the results obtained, the authors proposed the design chart presented in Figure 1 to adjust the volume loss associated with the 2T ($V_{s,2T}$), using the value obtained in greenfield conditions for the 1T excavated ($V_{s,1T}$) as reference. The correction factor reached a maximum of about 25% for the lowest P/D analyzed and then gradually decreased as the distance between tunnels increased, becoming negligible for P/D ratios greater than 7. Addenbrooke and Potts [16] also observed that the 2T settlement trough presented an eccentricity towards the 1T and proposed a correction (Figure 1) to determine the offset of the maximum settlement of the 2T Gauss curve (e_{2T}) as a function of the tunnel spacing (d).

Also based on a numerical study and supported by a series of 1g 1/50 small-scale models, Chapman et al. [22] and Hunt [39] proposed the introduction of a modification factor, F, on the 2T Gauss curve in order to include the interaction effects (Equation (4)).

$$\delta_{v,2T}(x) = F \cdot \delta_{v,max} \cdot e^{\left(-\frac{(x-d)^2}{2 \cdot i^2}\right)} \quad (4)$$

The modification factor is defined by Equation (5) and decreases linearly between a maximum value (1.6 to 1.8), directly above the centerline of the 1T, and 1.0 as the distance from the 1T centerline increases. In Equation (5), the parameter A corresponds to a multiple of the trough width parameter in a half settlement trough and is commonly set as 2.5 or 3 (with 3.0 adopted in this paper), while M is the maximum modification factor, varying between 0.6 and 1.5, with the value of 0.6 having been recommended by Hunt [39].

$$F = \left[1 + \left(M \cdot \left(1 - \frac{d + x}{A \cdot i}\right)\right)\right] \quad (5)$$

However, according to Hunt [39], the modification factor should only be applied in the "overlapping zone" of the two settlement troughs, where the soil is assumed to have been disturbed by the excavation of the 1T (Figure 2). This correction results in an asymmetric settlement trough, with the maximum settlement of the 2T presenting some eccentricity towards the 1T, as suggested by Addenbrooke and Potts [16].

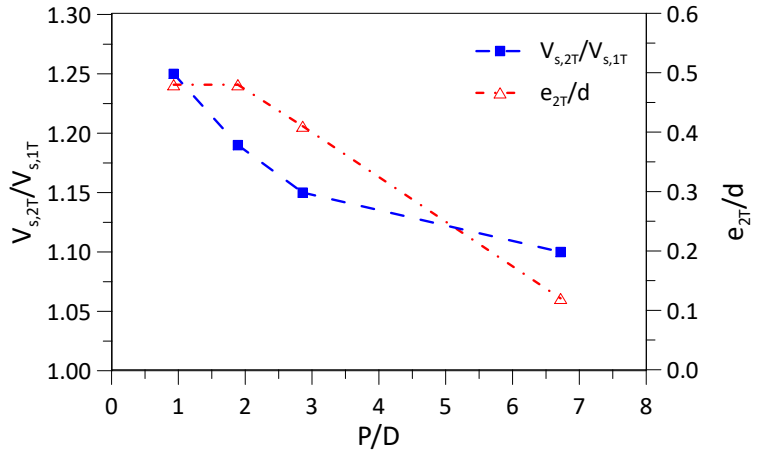

Figure 1. Design chart proposed by Addenbrooke and Potts [16] (replotted using the original data).

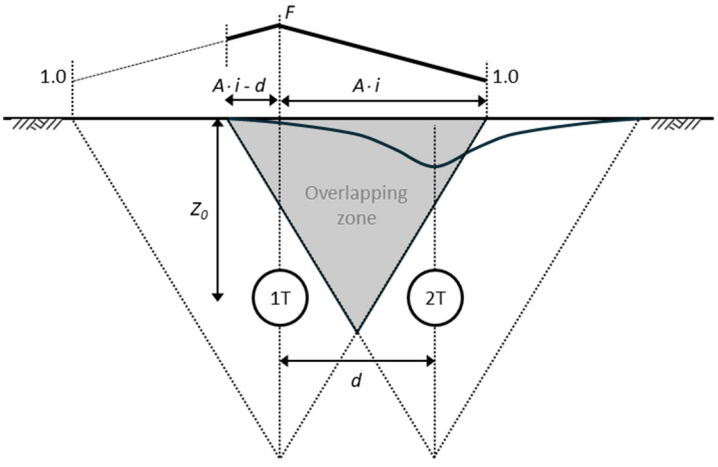

Figure 2. Overlapping zone according to Hunt [39] (modified from Hunt [39]).

Divall [55] investigated the interaction of side-by-side twin tunnels through a series of centrifuge tests. Based on their findings, the authors proposed a method similar to that presented by Addenbrooke and Potts [16], where the volume loss of the 2T ($V_{s,2T}$) was determined using the greenfield results (volume loss of the 1T) and the distance between the tunnels (d) as reference. The additional volume loss ($\Delta V_{s,2T}$) induced by the 2T excavation can be calculated using Equation (6), while the volume loss of the 2T can be obtained by adding the additional volume loss to the volume loss induced by the 1T, as expressed in Equation (7). Also, in this case, when the distance between the centerlines of the tunnels increases, the interaction effect reduces and becomes negligible for $d/D > 5.0$.

$$\Delta V_{s,2T} = 0.441 \cdot \left(\frac{d}{D}\right)^{-1.062} \cdot V_{s,1T} \tag{6}$$

$$V_{s,2T} = V_{s,1T} + \Delta V_{s,2T} \tag{7}$$

Although the maximum settlement was aligned with the centerline of the 2T, Divall and Goodey [4] observed an asymmetry in the shape of the 2T settlement trough, with the side towards the 1T being wider when the tunnels were closely spaced, likely due to the soil disturbance in that zone, as noted by Mair and Taylor [7]. To account for this effect, Divall [55] proposed a correction to the dimensionless trough width factor (K), suggesting that in the side towards the 1T (inside zone), a value of 0.7 should be adopted for distances between the centerlines of the tunnels smaller than 3D. In contrast, for the outside zone, the value obtained for greenfield conditions should be applied, regardless of the distance between tunnels. However, it should be noted that applying the correction proposed by Divall [55] results in a 2T volume loss greater than that calculated using Equations (6) and (7) since the settlement trough becomes wider in the inside zone, leading to an apparent inconsistency in the method.

Using the construction data of the excavation of the Otogar–Kirazli line of the Istanbul Metro as reference, Ocak [37] proposed a new analytical method for predicting settlements induced by twin tunnelling. Similarly to the modification factor proposed by Chapman et al. [22] and Hunt [39], Ocak [37] introduced a disturbance factor (k) to adjust the settlement trough induced by the 2T excavation. The disturbance factor, defined in Equation (8), is a function of the ratio between the distance between the tunnel centerlines and the tunnel diameter (d/D).

$$k = 1 + \frac{D}{d} \tag{8}$$

According to Ocak [37], both the trough width parameter and the maximum settlement associated with the 2T excavation should be multiplied by the disturbance factor, as expressed in Equations (9) and (10). In this method, similarly to previous methods, the final settlement trough can be obtained by adding the adjusted 2T curve to the settlement curve predicted for greenfield conditions (1T).

$$i_{2T} = k \cdot i \tag{9}$$

$$\delta_{v,2T}(x) = k \cdot \delta_{v,max} \cdot e^{\left(-\frac{(x-d)^2}{2 \cdot i_{2T}^2}\right)} \tag{10}$$

Using the field data of a twin tunnel excavation in Wuhan as reference, Zhou et al. [38] proposed a method very similar to that proposed by Chapman et al. [22] and Hunt [39], with the main difference being that instead of a linear decrease in the modification factor, Zhou et al. [38] adopted the exponential function expressed in Equation (11).

$$F = M \cdot \left(e^{-\frac{x^2}{2 \cdot i^2}} - 1 \right) \cdot \left(1 - e^{-\frac{(2 \cdot A \cdot i)^2}{8}} \right)^{-1} + 1 + M \quad (11)$$

In this expression, the parameters A and M are analogous to those defined by Chapman et al. [22], and Zhou et al. [38] recommends the adoption of similar values. Also, in this method, the modification factor should only be applied in the "overlapping" zone, as defined in Figure 2. The settlements induced by the 2T can then be calculated using Equation (4), with the final settlements being obtained as in the previous methods, i.e., by summing the adjusted 2T curve with the settlement curve predicted for greenfield conditions (1T).

More recently, Dong et al. [40] proposed a method where the settlements induced by the 2T were calculated by adding an additional curve that accounts for the soil disturbance caused by the 1T construction to the Gauss curve obtained in greenfield conditions. The authors proposed that this additional curve is located in the "overlapping" zone, centred above the midpoint between tunnels, and also follows a Gaussian shape. However, in this approach, the "overlapping" zone is established considering both the soil layering and the plastic zone that develops around the tunnel during excavation. This implies that applying the method requires prior knowledge of not just the soil stratification but also of the initial stress state and the strength parameters of all layers, making it cumbersome and impractical for early design assessments. Moreover, for the determination of the fitting parameters of the additional Gaussian curve, Dong et al. [40] assumed a linear relationship between the additional volume loss and the volume loss induced by the 1T. This assumption is inadequate, as it neglects the influence of tunnel spacing. It also implies that tunnels placed very close together or far apart would induce the same additional volume loss, which contradicts the findings from various case studies. For these reasons, it was decided not to consider this method in this study.

To compare the settlements predicted by the different analytical methods, a parametric study was conducted. For this purpose, twin tunnels with diameters (D) of 5 m, with their axis located at a depth (Z_0) of 20 m and spaced at distances (d) of 10, 20, and 30 m (corresponding to P/D ratios of 1.0, 3.0, and 5.0, respectively), were considered. It was assumed that the Gaussian curve in greenfield conditions (1T) had an i of 10m and a $\delta_{v,max-1T}$ of 10mm (equivalent to $V_s = 1.28\%$). The settlements normalized by the maximum settlement ($\delta_v/\delta_{v,max-1T}$) are plotted against the distance from the centre line of the 1T normalized by tunnel diameter (x/D) in Figure 3 for the three P/D ratios considered (check Table S1 for the dataset). The upper plots correspond to the predictions of the settlement induced by the 2T, while the lower plots represent the final settlements obtained after combining the settlements induced by both tunnels. The greenfield settlement (1T) is also superimposed in the plots for reference.

The results show that all methods predict that the settlement induced by the 2T increases as the P/D ratio decreases, except for the method proposed by O'Reilly and New [36], which assumes no interaction between tunnels. Consequently, in this method, the predicted settlements are in all cases equal to the greenfield ones. For a P/D = 1.0, the Ocak [37] method estimates an increase in the maximum settlement of about 50% compared to the reference value, whereas the other methods predict smaller increases ranging between 20 and 40%. As the P/D ratio increases, the predictions from all methods tend to become similar, with minimal interaction effects predicted for the P/D = 5.0 ratio, except for the methods of Addenbrooke and Potts [16] and Ocak [37]. Notably, Ocak's [37] method also estimates wider settlement curves, leading to significantly higher volume loss estimates. As for the eccentricity of the maximum settlement towards the 1T, the method proposed by Addenbrooke and Potts [16] clearly predicts the highest values. In contrast, the other methods generally predict minimal eccentricities, apart from Ocak [37] and Divall [55],

who do not consider any eccentricities. Naturally, as the P/D ratio increases, the predicted eccentricities decrease, and, by a ratio of 5.0, they become negligible in most methods, with the exception of the eccentricity predicted by the Addenbrooke and Potts [16] method.

The final settlements displayed in the lower plots of Figure 3 are a consequence of the predictions made for the 2T. As a result of the large eccentricities predicted by the Addenbrooke and Potts [16] method, very large settlement troughs for the higher P/D ratios considered (3.0 and 5.0) are predicted, with settlements being particularly higher across the entire pillar width between tunnels. For P/D = 1.0, the Ocak [37] method predicts the largest settlement trough, both in terms of maximum displacement and width. All other methods result in similar final settlement troughs, with the interaction effect between tunnels reducing as the P/D ratio increases. These results highlight the importance of the spacing between the tunnels in the prediction of the settlements induced by side-by-side twin tunnels.

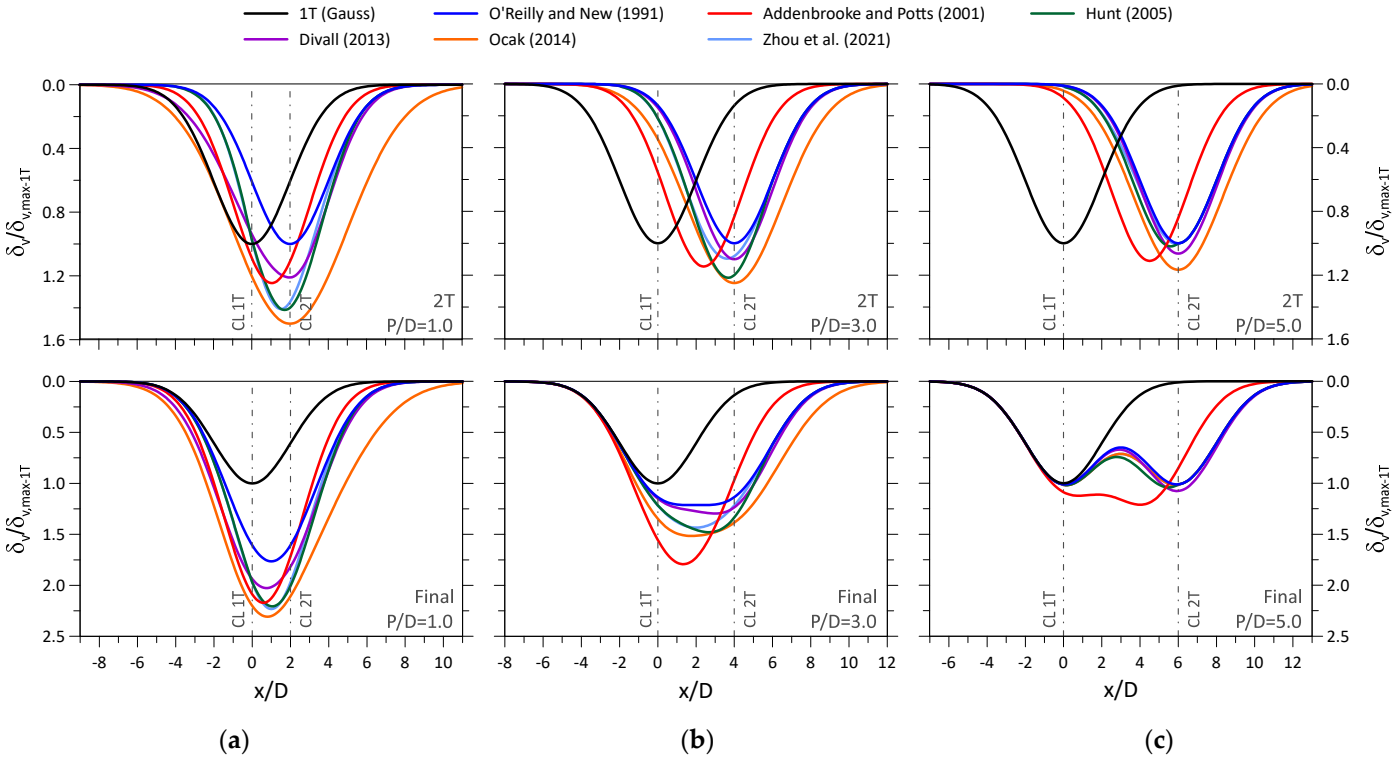

Figure 3. Comparison of the analytical methods proposed for the prediction of settlements induced by the 2T excavation for different pillar widths: (**a**) P/D = 1.0; (**b**) P/D = 3.0; (**c**) P/D = 5.0 [16,36–39,55].

2.2. Case Studies and Physical Model Tests

The analytical methods proposed in the literature were derived based on limited data, which were mainly obtained through numerical modelling and physical modelling or by analyzing the monitoring data of a small number of case studies. As a result, the reliability of the proposals is confined to specific scenarios, and their broader applicability has not yet been fully validated. However, with the increasing construction of underground transportation networks and the extensive dissemination tools available, there is now a vast number of cases studies in the literature, which reported quality monitoring data of settlements caused by side-by-side twin tunnelling excavations. A list of the collected case studies is presented in Table 1 and includes data from 19 projects, which encompass 46 sections where settlements were measured. Only cases where the tunnels and the monitoring alignments were perpendicular were considered in order to avoid any

effects related to the skew angle of the excavation, which are known to distort the typical Gaussian shape of the transverse settlement trough, making it asymmetrical [49]. Following the advances made in technology, it is not surprising that almost all tunnels were excavated using EPB shields, with only two projects identified as using sequential excavation. The ground conditions observed at the tunnel face varied significantly, ranging from medium stiff to stiff clays, silty soils (fine soil), granular materials, and soft rocks. The geometrical characteristics of the tunnels analyzed in the case studies are presented in Figure 4. The tunnel diameters ranged from 4.9 to 9.0 m, with the vast majority falling between 6.0 and 6.5 m. The depth to diameter ratio (Z_0/D) varied from 1.3 to 5.5, while the pillar width to diameter ratio (P/D) varies between 0.2 and 4.8, with most of the tunnels spaced 0.5 to 1.5 times their diameter apart. Overall, the geometrical space covered by the analyzed case studies is extensive, encompassing a wide range of P/D ratios.

Physical models of side-by-side twin tunnel excavations have also been reported in the literature. A total of four studies were identified, with their details summarized in Table 2. Of these, three studies involved small-scale models and one centrifuge test, totalizing eleven tests with available data. The geometrical space covered by these tests spans from Z_0/D values of 1.0 to 4.3, with P/D varying between 0.5 and 3.5. These tests have the advantage of being performed in a controlled environment, without the challenges associated with variable geological conditions and excavation operation factors. However, they present some limitations, such as the reduced stress state in the case of the small-scale models and the complexity of operating the centrifuge apparatus, in addition to the challenges associated with simulating the tunnel excavation mechanism, which differs in all studies.

Table 2. List of the physical models analyzed.

Source	Physical Model	Excavation Method	Soil	Test	Code	D (m)	Z_0 (m)	d (m)	P (m)
Divall et al. [56]	Centrifuge (100 g)	Support fluid	Speswhite kaolin clay	1	U1	4.00	10.00	6.00	2.00
				2	U2	4.00	10.00	12.00	8.00
				3	U3	4.00	10.00	18.00	14.00
Chapman et al. [25]	Small-scale (1/50)	Auger type cutter	Speswhite kaolin clay	A	V1	0.08	0.34	0.13	0.05
				B	V2	0.08	0.34	0.13	0.05
He et al. [27]	Small-scale (1/12)	EPB prototype	Synthetic	S-2	W	0.52	0.54	1.04	0.52
Zheng et al. [28]	Small-scale (1/60)	Shrinking tunnel	Sand	T1	X1	0.10	0.25	0.15	0.05
				T2	X2	0.10	0.25	0.15	0.05
				T3	X3	0.10	0.25	0.15	0.05
				T4	X4	0.10	0.25	0.30	0.20
				T5	X5	0.10	0.25	0.45	0.35

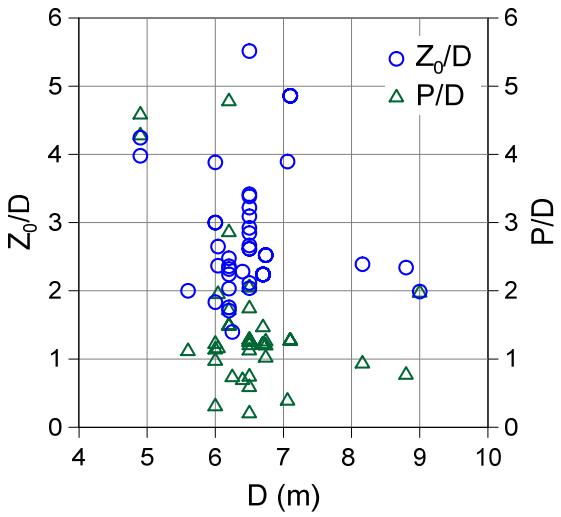

Figure 4. Geometrical characteristics of the twin tunnels analyzed in the case studies.

3. Results and Discussion

3.1. Adjustment of the Gaussian Curves to the Settlement Data

The initial step in predicting twin tunnel settlement using any analytical method involves adjusting a Gaussian curve that fits the settlements obtained in greenfield conditions, i.e., after the 1T excavation. In this study, there was no need to estimate the Gaussian parameters using empirical expressions since the results from the case studies and physical models presented in Tables 1 and 2 were available. In total, the settlements of the 57 listed sections were analyzed, and the parameters of the Gaussian curves ($\delta_{v,max-1T}$ and i_{1T}) were fitted by applying the least square method. The obtained parameters and corresponding fitting metrics are presented in Table A1 in Appendix A. In addition to the standard coefficient of determination (R^2), calculated using Equation (A1), the root mean squared error (RMSE) was also computed using Equation (A2), as this metric provides a more interpretable and practical assessment of the fit. To evaluate if the settlements induced by the 2T excavation also followed a Gaussian shape, as suggested by some of the analytical methods [13,38,57], the data from this excavation (obtained by subtracting the settlements of the 1T to the final ones measured) were also fitted using a similar approach. Figure 5a presents the R^2 obtained for both 1T and 2T excavations. It can be observed that the quality of the fit of the 1T data is significantly higher, with R^2 values exceeding 0.9 for almost all analyzed sections. In contrast, the fit of the 2T data is lower, with many sections presenting an R^2 below 0.9. In order to improve the fit of the 2T data, an additional parameter was introduced in the calibration of the Gaussian curve, so that the maximum displacement could exhibit some eccentricity (e_{2T}) toward the 1T (considered positive), as suggested by Addenbrooke and Potts [16] and Hunt [39]. It should be noted that in some sections (see note 2 in Table A1), the best fit was obtained with an eccentricity directed toward the lateral side (negative eccentricity). In these cases, where atypical movements were observed, a null eccentricity was considered in the analyses, even if it did not provide the optimal fit. The obtained results are presented in Table A1 (Appendix A), with the corresponding R^2 values displayed in Figure 5b. The results show a significant improvement in the fit, with the vast majority of sections reaching R^2 values above 0.9. A similar conclusion can be drawn from Figure 5c, where the RMSE of both excavations is depicted. With the introduction of free eccentricity, the quality of the fit improved considerably, with most sections presenting RMSE values below 0.15. The sections with poorer fits are indicated in the figure (D1, E1, G1, G5, J, N2, P, Q, and R1) and are all associated with atypical and/or asymmetrical movements observed on one of the lateral sides of the

tunnels. Overall, the results confirm that both the 1T and 2T excavation appears to be adequately described by a Gaussian curve, which, in the case of the 2T, is eccentric.

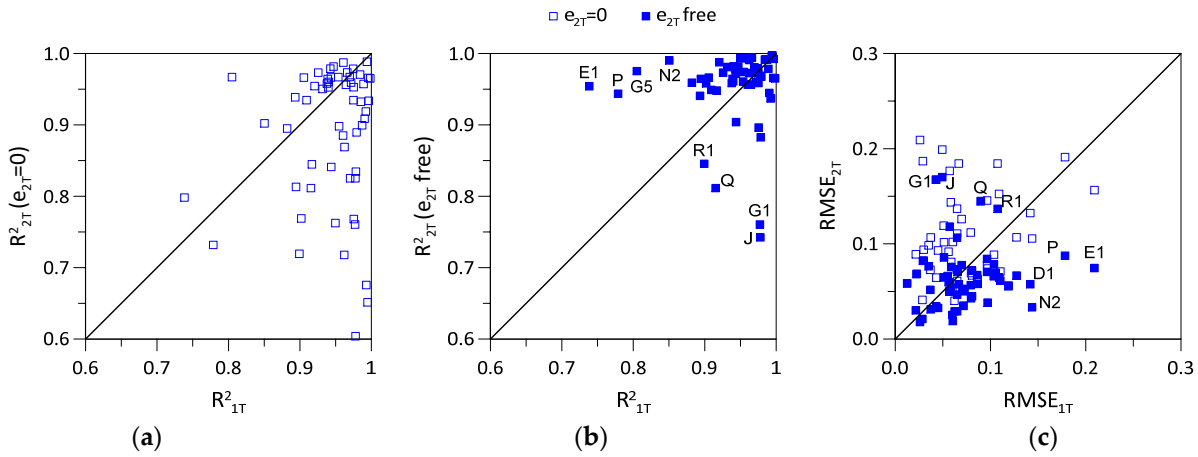

Figure 5. Metrics associated with the fitting of the Gaussian curves: (**a**) R^2 with no eccentricity; (**b**) R^2 with free eccentricity; (**c**) RMSE.

The fitted Gaussian parameters for both the 1T and 2T are compared in Figure 6, with the data grouped by soil type for the analyzed cases studies and into a group comprising all results from the physical models to facilitate the interpretation. According to the analytical methods, it should be expected that both the maximum settlement (Figure 6a) and the trough width parameter (Figure 6b) would be larger for the 2T excavation, leading to higher volume losses (Figure 6c). However, this is not the case in several sections, where the maximum settlement and, particularly, the trough width parameter are higher for the 1T excavation. As a result, in several sections (see note 15 in Table A1), the excavation of the 2T induced smaller volume losses than those observed in the 1T excavation. A detailed analysis of the studies where this condition occurred revealed two key factors that justify the results: (i) atypical movements recorded on one side of the tunnel and (ii) adjustments to shield operational parameters in the 2T excavation, such as face and grout pressure and penetration rate, which lead to smaller settlements (inclusively heave) and, consequently, smaller volume losses. This was the case observed in the Bangkok MRTA (case G) where Suwansawat and Einstein [13] highlighted the importance of controlling and adjusting the shield operational parameters in mitigating ground settlements. It is worth noting that no specific trend was observed regarding the type of soil, with anomalies identified in nearly all groups considered.

For comparison with the empirical estimation of the Gauss parameters associated in the 1T excavation, the trough width factor (K) and the volume loss (V_{s-1T}) are plotted in Figure 7 against the normalized tunnel axis depth. The trough width factor value (Figure 7a) ranges from 0.2 to 0.9, with the majority of the cases concentrated between 0.3 and 0.6, as indicated by Mair and Taylor [7]. Also in this case, there appears to be no clear relationship between the obtained K values and either the type of soil or the tunnel depth, although it should be noted that the soil stratification existent in almost all cases analyzed, and the different magnitude of settlements, which necessarily correspond to different deviatoric strains and stiffnesses in the soil, influence the results and difficult the establishment of a direct correlation. In terms of volume loss (Figure 7b) the results show that in the vast majority of the sections analyzed a value smaller than 1.0% is determined, regardless of the type of soil or tunnel depth. The case studies where the volume loss exceeds 1.0% correspond to specify projects where (i) an open shield (E2) was used; (ii) inappropriate operational shield parameters were adopted (A, G1, G2 and G5); (iii) difficult ground conditions (L3, H1 and H3); (iv) tail void closure was faulty (C and E1). In the

physical models the volume loss is imposed, with values above 1.0% being adopted in all cases. As a result, it appears adequate and conservative to adopt a volume loss of 1.0% as reference, provided that the excavation is carried out in a controlled manner.

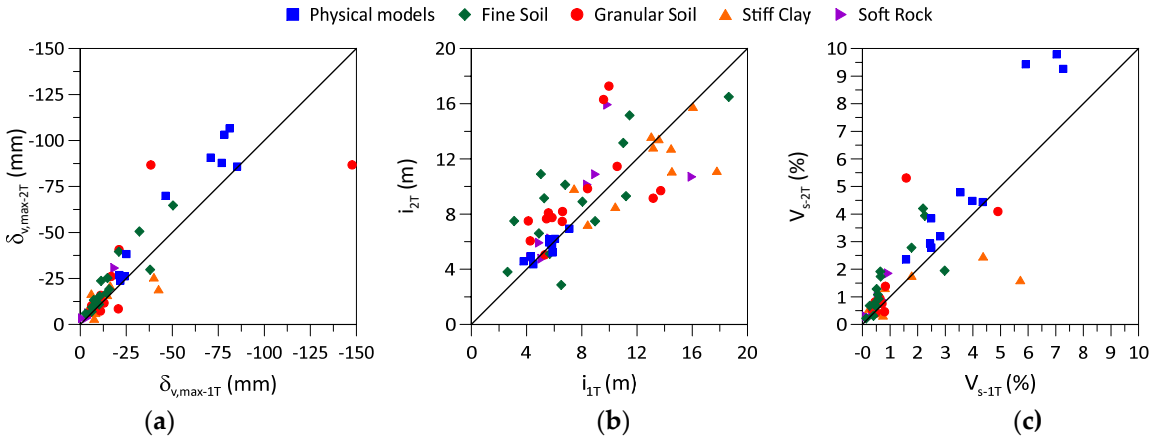

Figure 6. Comparison of the fitted Gaussian parameters for the 1T and 2T: (**a**) $\delta_{v,max}$; (**b**) i; (**c**) V_s.

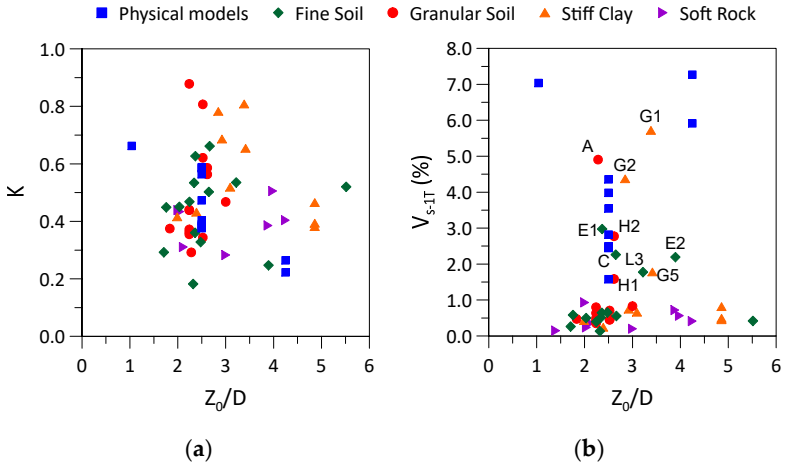

Figure 7. Influence of the depth of the tunnel axis on the 1T excavation: (**a**) trough width factor; (**b**) volume loss.

Figure 8 presents the Gaussian parameters derived for 2T excavation plotted against the pillar width ratio (P/D). Both the trough width parameter and the volume loss exhibit significant scatter across all P/D ratios, with no discernible trend. Moreover, the parameters obtained also appear to be uncorrelated with the type of soil or test. In the case of normalized eccentricity, while visible scatter is present, its value tends to decrease for larger P/D ratios. It is also possible to verify that the proposal by Addenbrooke and Potts [16] clearly overestimates the eccentricity values, with just a single section (case P) exhibiting an eccentricity of similar magnitude.

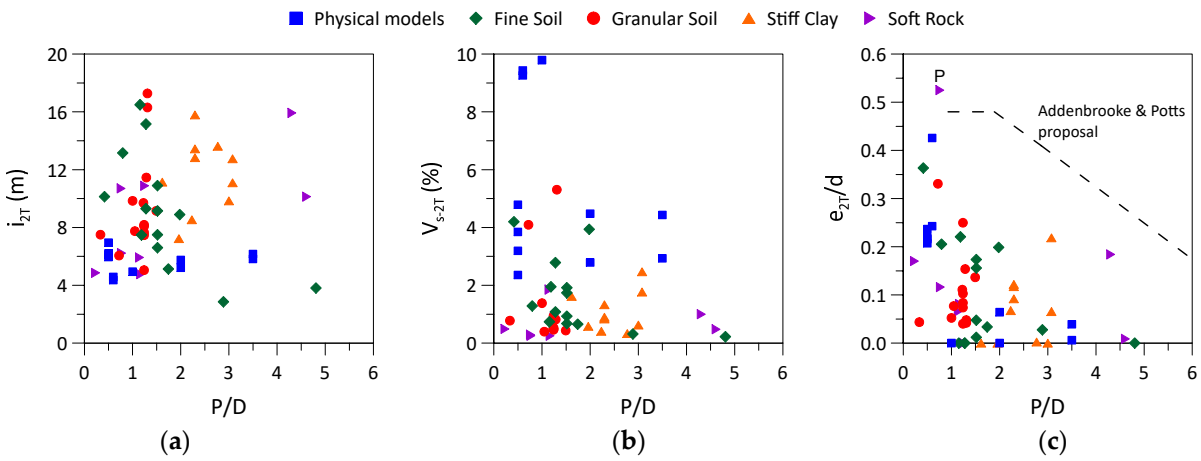

Figure 8. Influence of the pillar width on the 2T excavation: (**a**) i; (**b**) V_s; (**c**) e/d [16].

3.2. Assessment of the Analytical Methods

The evaluation of the settlement predictions induced by the 2T excavation using analytical methods was performed using the Gaussian parameters derived for the 1T and is presented in Table A1. For this evaluation, only 35 out of the 46 initial cases were considered, since the cases where the volume loss induced by the 2T excavation was smaller than that induced by the 1T excavation were excluded, as these are atypical and not covered by the analytical methods. In the assessment, only the RMSE (Equation (A2)) was employed, as this metric is more suitable for evaluating the quality of the fit.

Figure 9 shows the RMSE calculated for each case across all methods for both the 2T and final settlements. The horizontal dashed lines represent the average RMSE obtained for each method, considering all cases. Since the quality of the fit of the 1T excavation is very high in all cases, the RMSE values obtained for both the 2T and final settlements are very similar, as can be seen in the figure. Despite some scatter, the RMSE values are generally small in most cases. As expected, the cases where the RMSE is higher correspond to some of the cases previously identified as exhibiting atypical movements. On average the method proposed by Addenbrooke and Potts [16] produces the poorest results, with RMSE values being even higher than those from the O'Reilly and New [36] method, where no interaction effects between tunnels were considered. This poor performance is justified by the excessive eccentricity of the maximum settlement predicted by the Addenbrooke and Potts [16] method, as observed in Figure 8c. All other methods produce smaller average RMSE values, with small differences between them. The method with the lowest average RMSE is the one proposed by Hunt [39], followed closely by the methods of Divall [55], Zhou et al. [38], and Ocak [37]. For these four methods, the RMSE value is plotted against the P/D ratio in Figure 10. In all cases, the quality of the fit improves with higher P/D ratios. For P/D ratios between 0.5 and 2.0, significant scatter is observed, with the Ocak [37] method displaying a higher concentration of RMSE values between 0.2 and 0.6. Across all methods, no clear relationship is observed between the soil type and the quality of the fit.

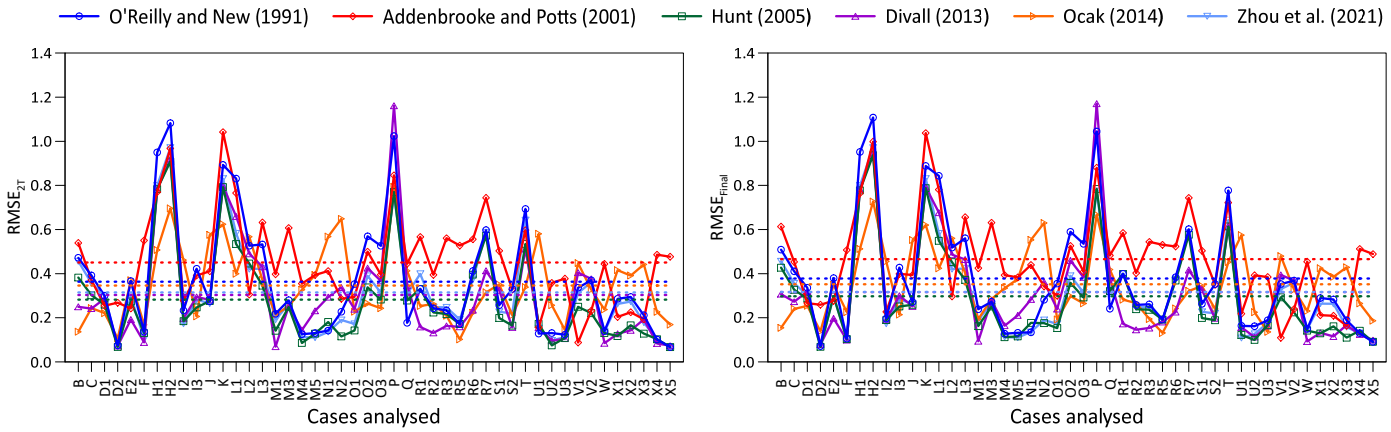

Figure 9. Assessment of the predictions made by the analytical methods for the analyzed cases: (**a**) 2T settlements; (**b**) final settlements [16,36–39,55].

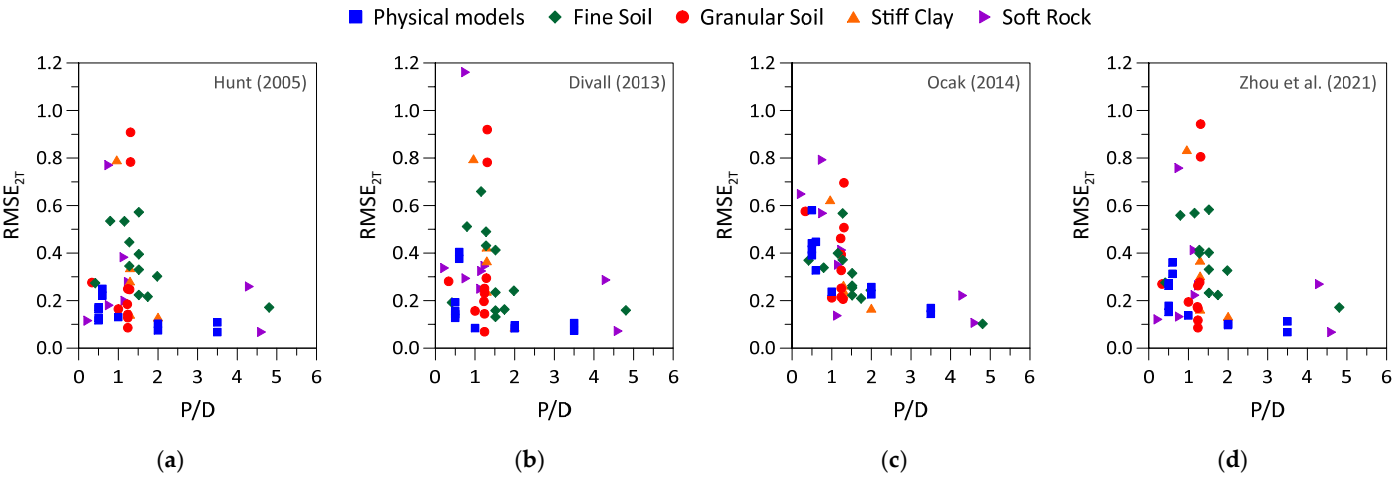

Figure 10. Assessment of the predictions made by the analytical methods as a function of P/D ratio: (**a**) Hunt [39]; (**b**) Divall [55]; (**c**) Ocak [37]; (**d**) Zhou et al. [38].

As previously mentioned, the methods proposed by Hunt [39] and Zhou et al. [38] allow for some flexibility regarding the interaction between tunnels. This flexibility is governed by the maximum modification factor (M), which, according to Hunt [39], varies between 0.6 and 1.5, with this study adopting the value of 0.6, as recommended by Hunt [39]. To evaluate the influence of this parameter, an additional optimization study was performed in which M was adjusted to minimize the RMSE. In this analysis, an interval for M ranging from 0 (no interaction effects) to 3 was explored, expanding the interval proposed by Hunt considerably [39]. The comparison of the RMSE with fixed and free M is presented in Figure 11a for both the Hunt [39] and Zhou et al. [38] methods. As expected, for both methods, an improvement in the fit was observed, with a corresponding reduction in the RMSE. However, in the majority of cases, the reduction in RMSE was limited to less than 15%. The optimized M values are presented in Figure 11b for both methods. The obtained values vary significantly across the explored range, with no clear trend observed. Clearly, in the method proposed by Zhou et al. [38], the best fit would occur for values above 3.0, which are already double the maximum value of 1.5 suggested by Hunt [39]. The range of M values obtained, coupled with the limited RMSE reduction observed suggest that the settlements are not strongly dependent on M.

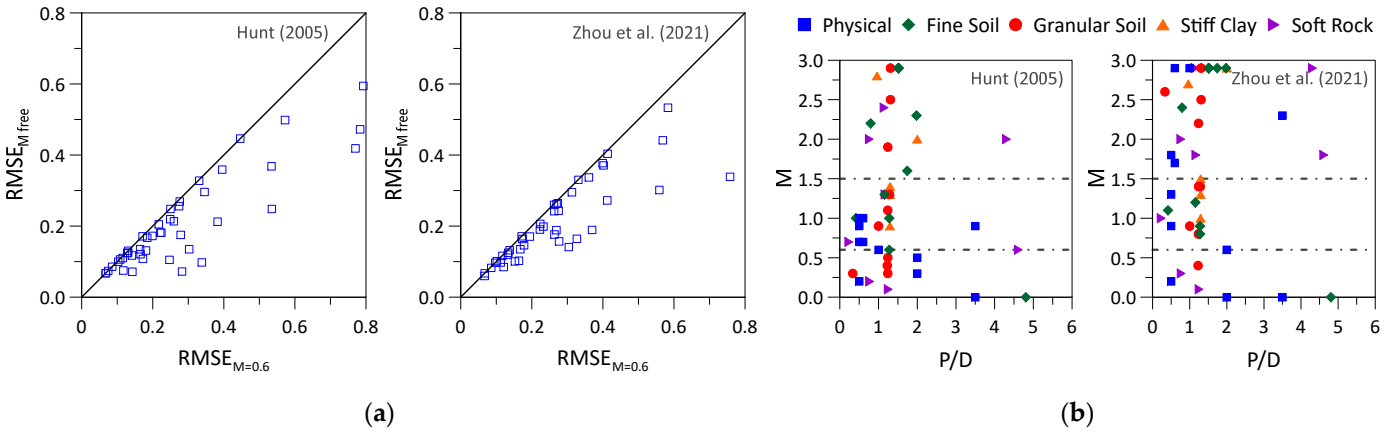

Figure 11. Influence of the maximum modification factor employed in Hunt [39] and Zhou et al. [38] methods: (**a**) RMSE; (**b**) pillar width.

To illustrate the application of the methods to the analyzed case studies, the settlements determined for the 2T excavation, along with the final settlements obtained by adding these to the greenfield results (1T), are presented in Figure 12 for cases N1, R6, and D2 (check Table S1 for the dataset). These cases were selected since they represent distinct P/D ratios—0.8, 1.5, and 4.6, respectively—covering a range from closely spaced tunnels to tunnels located spaced apart. The results show that a reasonable adjustment is achieved for the smallest P/D ratio (case N1), with most methods adequality predicting the 2T excavation and final displacements. The exceptions are the Addenbrooke and Potts [16] and Ocak [37] methods, with the former predicting a Gaussian distribution with excessive eccentricity, while the later estimates a high settlement and a significantly wider settlement trough. The poorest fit is observed for the intermediate P/D ratio (case R6). In this case, only the method proposed by Divall [55] provides a good fit, successfully predicting the higher displacements occurring on the pillar width side. The Addenbrooke and Potts [16] and Ocak [37] methods exhibit the same issues previously described, while the other methods underpredict the settlements. The case with the highest P/D ratio (case D2) presents the more accurate predictions, with almost all methods estimating that, for tunnels spaced so far apart, minimal interaction occurs. The exception is the prediction by the Addenbrooke and Potts [16] method, which performs poorly due to the excessive eccentricity estimated for the 2T excavation. For these particular cases, the Divall [55] method corresponded to the best fit. However, overall, as mentioned previously, the Hunt [39] method provides the most reliable prediction across all cases analyzed.

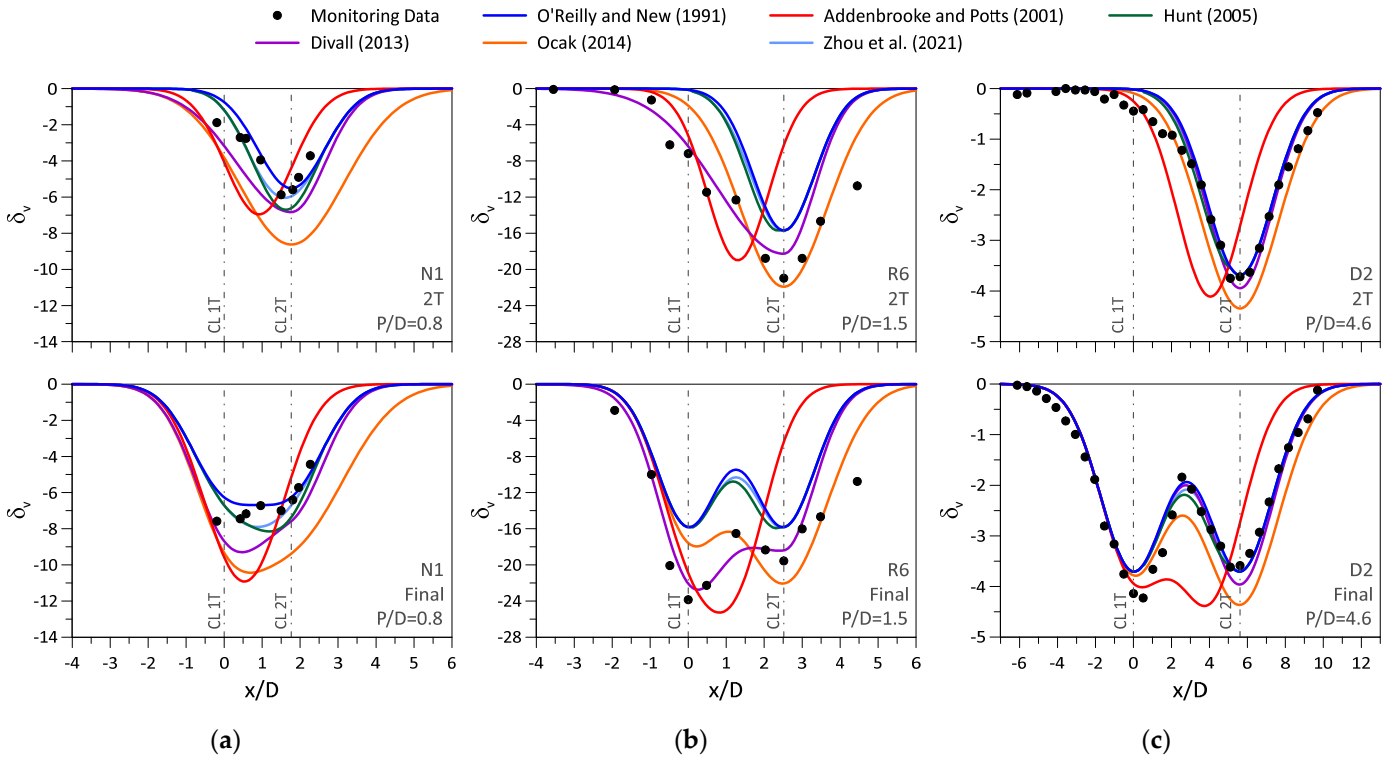

Figure 12. Settlements predicted for the 2T by the analytical methods for three cases analyzed (**a**) N1; (**b**) R6; (**c**) D2 [16,36–39,55].

4. Conclusions

Twin tunnelling in urban centres is becoming increasingly common, creating a growing need to quickly and accurately assess the impact of the excavation-induced settlements in the structures at ground surface. In this context, the use of simplified methods to adequately predict those settlements is fundamental. This paper describes the methods proposed in the literature and assesses their performance by comparing their predictions with monitoring data from 57 sections documented in previous studies. Based on the results, the following conclusions can be drawn:

1. All methods assume that the excavation of both the 1T and 2T induces a Gaussian settlement trough. With the exception of the O'Reilly and New [36] method, which does not account for tunnel interaction, all other methods predict that the 2T excavation induces higher settlements, with this increase being a function of the tunnel's proximity;
2. The methods differ in how they account for the interaction effects: Addenbrooke and Potts [16] and Divall [55] suggest a correction for the volume loss (with an additional eccentricity correction in the case of the former); Hunt [39] and Zhou et al. [38] propose the application of a corrective factor in the "overlapping zone" between both tunnels; and Ocak [37] suggests a correction factor applied to both the Gaussian parameters (maximum displacement and trough width);
3. The fitting of the monitoring data to the analyzed case studies confirmed that the settlements induced by the 1T are very adequately described by a Gaussian curve. However, for the settlements induced by the 2T, a very good fit was only achieved if an eccentric Gaussian curve was considered. This confirms that the superposition method of two Gaussian curves is appropriate for predicting the settlements induced by twin tunnelling;

4. Despite the very good fit, the obtained Gaussian parameters exhibit significant scatter across all valid sections, and no clear trend was possible to establish in relation to either the soil type or the dimension of the pillar width;
5. The application of the analytical methods to predict the monitoring data revealed that the Addenbrooke and Potts [16] proposal performs very poorly due to the application of the eccentricity correction, performing even worse than the O'Reilly and New [36] method. The remaining methods predict the induced settlements of the 2T excavation with similar accuracy, with the Hunt [39] proposal being slightly more reliable across all cases, regardless of the soil type or the dimension of the pillar width;
6. The maximum modification parameter adopted by the Hunt [39] and Zhou et al. [38] methods to improve the 2T settlement prediction has a limited impact on the results, with improvements generally below 15%.

These results show that the existing analytical methods, with the exception of the Addenbrooke and Potts [16] and O'Reilly and New [36] proposals, can be used to predict, with reasonably accuracy, the settlements associated with twin tunnelling during the early stages of design, across all ranges of soil types and P/D ratios. However, when tested against real case scenarios, all methods exhibited limitations that are inherent to the ground variability and the complexity associated with tunnel excavation process. Factors such as challenging ground conditions and inadequate operational shield parameters can induce substantial ground movements that cannot be predicted by simple analytical methods, which are only applicable to simple scenarios.

Supplementary Materials: The following supporting information can be downloaded at www.mdpi.com/xxx/s1. Table S1. Dataset of the results of the application of the analytical methods in different case scenarios.

Author Contributions: Conceptualization, A.M.G.P. and J.C.D.G.; methodology, A.M.G.P.; data curation, A.M.G.P.; validation, J.C.D.G. and J.A.e.S.; writing—original draft preparation, A.M.G.P.; writing—review and editing, J.C.D.G. and J.A.e.S. All authors have read and agreed to the published version of the manuscript.

Funding: This work was partly financed by FCT/MCTES through national funds (PIDDAC) under the R&D Unit Institute for Sustainability and Innovation in Structural Engineering (ISISE), under reference UIDB/04029/2020, and under the Associate Laboratory Advanced Production and Intelligent Systems ARISE under reference LA/P/0112/2020.

Institutional Review Board Statement: Not applicable.

Informed Consent Statement: Not applicable.

Data Availability Statement: The original contributions presented in this study are included in the article/supplementary material. Further inquiries can be directed to the corresponding author.

Conflicts of Interest: Author José C. D. Grazina is employed by the company Infraestruturas de Portugal. The remaining authors declare that the research was conducted in the absence of any commercial or financial relationships that could be construed as a potential conflict of interest.

Appendix A

The metrics employed in the assessment of the analytical solutions were the coefficient of determination (R^2) and the root mean squared error ($RMSE$), which are given by Expressions (A1) and (A2), respectively:

$$R^2 = 1 - \frac{\sum_{i=1}^{N_{obs}} \left(\delta_{v,observed,i} - \delta_{v,predicted,i}\right)^2}{\sum_{i=1}^{N_{obs}} \left(\delta_{v,observed,i} - \overline{\delta_{v,observed,i}}\right)^2} \quad \text{(A1)}$$

$$RMSE = \sqrt{\frac{\sum_{i=1}^{N_{obs}} \left(\frac{\delta_{v,predicted,i}}{\delta_{v,max-1T}} - \frac{\delta_{v,observed,i}}{\delta_{v,max-1T}}\right)^2}{N_{obs}}} \quad \text{(A2)}$$

where N_{obs} is the number of data points reported for each case analyzed. The terms $\delta_{v,predicted,i}$ and $\delta_{v,observed,i}$ refer to the settlements determined by the analytical solutions and those observed in the cases analyzed, respectively, while $\delta_{v,observed,i}$ corresponds to the mean of the observed values and $\delta_{v,max-1T}$ to the Gaussian parameter for greenfield conditions (1T).

Table A1 presents the Gaussian parameters fitted for all cases analyzed in the excavation of both 1T and 2T, along with the corresponding metrics (R^2 and *RMSE*), auxiliary variables, and notes regarding the fitting.

Table A1. Gaussian parameters fitted to the cases studies and physical models analyzed.

	Fitting of the 1T							Fitting of the 2T							
Code	$\delta_{v,max}$ **(mm)**	i **(m)**	V_s **(%)**	**R²**	**RMSE (mm)**	**K**	**e2T (m)**	$\delta_{v,max}$ **(mm)**	i **(m)**	V_s **(%)**	**R²**	**RMSE (mm)**	**e2T/d**	$V_{s,1T}/V_{s,2T}$	**Notes**
A	−147.68	4.26	4.91	0.99	3.85	0.29	−3.64	−86.73	6.06	4.09	1.00	1.56	0.33	0.83	(1) (15)
B	−18.63	4.92	0.93	0.93	1.48	0.44	−0.79	−30.69	5.93	1.85	0.98	1.31	0.07	1.99	
C	−32.14	8.04	2.26	0.90	3.51	0.50	−3.58	−50.59	8.90	3.94	0.96	3.28	0.20	1.74	
D1	−4.30	9.86	0.56	0.89	0.61	0.51	−4.79	−4.72	15.93	1.00	0.96	0.27	0.18	1.77	(3)
D2	−3.69	8.40	0.41	0.97	0.21	0.40	−0.24	−3.56	10.13	0.48	0.98	0.18	0.01	1.16	
E1	−37.96	8.96	2.98	0.74	7.94	0.63	−2.91	−29.79	7.48	1.95	0.95	2.22	0.22	0.66	(3) (15)
E2	−50.39	6.80	2.19	0.97	2.94	0.25	−3.63	−64.73	10.13	4.20	0.98	3.47	0.36	1.92	
F	−14.65	7.45	0.43	0.98	0.96	0.42	0.00	−16.11	9.84	0.62	0.97	1.14	0.00	1.45	(2)
G1	−42.57	17.78	5.72	0.98	1.82	0.81	0.00	−19.17	11.14	1.61	0.76	3.21	0.00	0.28	(2) (5) (7) (15)
G2	−39.99	14.47	4.37	0.92	3.86	0.78	−4.37	−25.63	12.76	2.47	0.95	2.16	0.22	0.56	(8) (15)
G3	−7.57	13.04	0.75	0.93	0.54	0.69	−0.04	−3.20	13.62	0.33	0.97	0.17	0.00	0.44	(7) (15)
G4	−8.37	10.43	0.66	0.97	0.50	0.52	−0.98	−6.36	8.53	0.41	0.99	0.16	0.07	0.62	(8) (15)
G5	−16.23	14.52	1.78	0.80	1.79	0.65	−1.31	−21.08	11.10	1.77	0.98	1.29	0.07	0.99	(13) (15)
H1	−21.06	9.96	1.58	0.89	2.50	0.59	−0.63	−40.67	17.27	5.31	0.94	2.25	0.04	3.35	
H2	−38.35	9.58	2.77	0.94	3.09	0.56	−0.72	−86.70	16.30	10.68	0.96	6.22	0.05	3.85	(12)
I1	−10.96	5.84	0.45	0.99	0.33	0.34	−1.06	−7.28	7.75	0.40	0.94	0.60	0.08	0.88	(15)
I2	−7.33	13.72	0.71	0.92	0.71	0.81	−1.66	−11.06	9.70	0.75	0.99	0.42	0.11	1.07	
I3	−6.13	10.56	0.45	1.00	0.13	0.62	−2.37	−10.13	11.46	0.82	0.99	0.31	0.15	1.79	
J	−12.91	4.12	0.47	0.98	0.64	0.37	−0.35	−11.67	7.50	0.78	0.74	1.99	0.04	1.64	(4)
K	−6.00	8.43	0.24	1.00	0.14	0.43	0.00	−16.76	7.23	0.58	0.97	1.15	0.00	2.40	(2)
L1	−2.96	18.65	0.42	0.95	0.18	0.52	0.00	−5.91	16.50	0.74	0.99	0.11	0.00	1.76	(2)
L2	−6.44	11.46	0.56	0.95	0.46	0.66	0.00	−9.44	15.16	1.08	0.98	0.33	0.00	1.94	(2)
L3	−20.98	11.20	1.78	0.94	1.52	0.54	0.00	−39.61	9.30	2.78	0.98	1.99	0.00	1.57	(2)
M1	−7.47	6.60	0.35	0.99	0.28	0.44	−1.11	−9.18	8.18	0.53	0.98	0.47	0.07	1.52	
M2	−20.65	5.44	0.80	0.99	0.60	0.36	−3.75	−8.46	7.66	0.46	0.94	0.69	0.25	0.58	(9) (15)
M3	−16.77	5.32	0.63	0.97	1.09	0.35	−0.60	−26.11	5.05	0.94	0.98	1.22	0.04	1.48	
M4	−8.78	6.58	0.41	0.98	0.49	0.44	−1.54	−9.24	7.47	0.49	0.97	0.55	0.10	1.19	
M5	−10.09	5.58	0.40	0.99	0.35	0.37	−1.25	−8.43	8.09	0.48	0.94	0.64	0.08	1.21	
M6	−5.28	13.17	0.49	0.96	0.34	0.88	−2.28	−6.69	9.15	0.44	0.99	0.19	0.14	0.88	(11) (15)
N1	−5.51	5.75	0.24	0.98	0.28	0.43	−1.34	−5.41	6.23	0.25	0.88	0.46	0.12	1.06	
N2	−11.13	4.27	0.36	0.85	1.60	0.31	−1.36	−13.35	4.86	0.49	0.99	0.45	0.17	1.36	(5)
O1	−8.03	16.05	0.82	0.96	0.50	0.47	−1.50	−13.27	15.79	1.33	0.99	0.39	0.09	1.62	
O2	−5.39	13.17	0.45	0.98	0.23	0.38	−1.99	−10.27	12.84	0.83	0.99	0.35	0.12	1.86	
O3	−5.74	13.58	0.49	0.99	0.16	0.39	−1.91	−10.50	13.44	0.89	1.00	0.22	0.12	1.81	
P	−1.13	15.97	9.15	0.78	0.20	1.83	−5.78	−3.33	10.70	0.29	0.94	0.29	0.53	1.97	(3)

Q	−9.03	8.99	0.72	0.92	0.81	0.39	0.00	−9.15	10.89	0.88	0.81	1.33	0.00	1.23	(2) (6)
R1	−10.24	3.10	0.26	0.90	1.10	0.29	−2.43	−10.88	7.50	0.68	0.85	1.49	0.16	2.57	(4)
R2	−14.35	4.89	0.58	0.98	0.82	0.45	−2.71	−16.97	6.61	0.93	0.90	2.00	0.17	1.60	
R3	−10.56	5.68	0.50	0.94	1.02	0.45	−0.57	−15.37	5.13	0.65	0.96	1.09	0.03	1.32	
R4	−7.34	6.51	0.40	0.95	0.63	0.47	−0.67	−13.24	2.86	0.31	0.96	0.89	0.03	0.79	(14) (15)
R5	−6.19	2.62	0.13	0.91	0.64	0.18	0.00	−6.95	3.81	0.22	0.97	0.46	0.00	1.63	(2)
R6	−15.69	5.04	0.66	0.94	1.66	0.33	−0.19	−19.19	10.90	1.74	0.96	1.33	0.01	2.65	
R7	−14.78	5.27	0.65	0.98	0.87	0.36	−0.74	−25.24	9.15	1.92	0.96	1.91	0.05	2.97	
S1	−4.43	5.09	0.20	0.94	0.29	0.28	−1.06	−6.03	4.77	0.25	0.90	0.64	0.08	1.27	
S2	−11.11	8.42	0.83	0.94	0.96	0.47	−0.63	−15.82	9.84	1.38	0.97	0.92	0.05	1.67	
T	−11.27	11.00	0.51	0.95	0.89	0.53	−3.24	−23.69	13.16	1.28	0.97	1.34	0.21	2.51	(10)
U1	−24.17	5.85	2.82	0.88	3.08	0.58	−1.42	−26.18	6.12	3.19	0.96	1.75	0.24	1.13	(16)
U2	−21.23	5.88	2.49	0.94	1.71	0.59	−0.77	−26.81	5.21	2.79	0.98	1.20	0.06	1.12	(16)
U3	−21.74	5.64	2.45	0.91	2.25	0.56	−0.70	−23.84	6.17	2.93	0.95	1.87	0.04	1.20	(16)
V1	−81.15	4.49	7.27	0.96	5.42	0.26	−2.73	−106.56	4.36	9.26	0.97	6.13	0.43	1.27	(16)
V2	−78.30	3.79	5.92	0.99	2.92	0.22	−1.55	−103.18	4.58	9.43	0.99	3.22	0.24	1.59	(16)
W	−200.03	4.29	7.04	1.00	2.50	0.66	0.00	−241.69	4.94	9.79	0.97	14.12	0.00	1.39	(2) (16)
X1	−25.08	7.10	1.58	0.99	1.13	0.47	−1.87	−38.26	6.95	2.36	0.99	1.25	0.21	1.49	(16)
X2	−46.36	6.06	2.49	0.98	2.36	0.40	−1.98	−69.93	6.21	3.85	0.97	4.52	0.22	1.55	(16)
X3	−70.84	5.65	3.55	0.96	4.93	0.38	−1.94	−90.68	5.96	4.79	0.96	7.04	0.22	1.35	(16)
X4	−76.87	5.84	3.98	0.96	4.98	0.39	0.00	−87.82	5.75	4.48	0.96	6.41	0.00	1.12	(2) (16)
X5	−85.20	5.77	4.36	0.97	4.70	0.38	−0.16	−85.83	5.83	4.43	0.96	5.64	0.01	1.02	(2) (16)

(1) Improvements in shield design during the 2T excavation. (2) In the fitting of the 2T, the eccentricity was considered to be 0. (3) Settlement trough of 1T is asymmetric, with the limb towards the 2T side showing atypical movements. (4) Settlement trough of the 2T shows atypical movements in the limb towards the 1T side. (5) Settlement trough of the 1T shows atypical movements in the limb away from the 2T side. (6) Settlement trough of the 2T presents significant scatter. (7) Higher face pressure and penetration rate of the EPB during 2T excavation. (8) Higher face and grout pressure of the EPB during 2T excavation. (9) Very small displacements induced by the 2T despite the smaller face pressure applied by the EPB. (10) The maximum settlement above the 1T was not measured at its centerline but at 0.5D towards the 2T. (11) No monitoring data available near the centerline of the 1T. (12) No monitoring data available near the centerline of the 2T. (13) No monitoring data available near the centerline of the 1T, and the grout pressure applied in 2T was much higher. (14) Heave was induced by the 2T excavation above the pillar width. (15) Volume loss induced by the 2T excavation is higher than that determined for the 1T. (16) Values obtained after applying the geometric scale of the model.

References

1. Admiraal, H.; Cornaro, A. Why underground space should be included in urban planning policy—And how this will enhance an urban underground future. *Tunn. Undergr. Space Technol.* **2016**, *55*, 214–220. https://doi.org/10.1016/j.tust.2015.11.013.
2. Bobylev, N. Underground space as an urban indicator: Measuring use of subsurface. *Tunn. Undergr. Space Technol.* **2016**, *55*, 40–51. https://doi.org/10.1016/j.tust.2015.10.024.
3. Broere, W. Urban underground space: Solving the problems of today's cities. *Tunn. Undergr. Space Technol.* **2016**, *55*, 245–248. https://doi.org/10.1016/j.tust.2015.11.012.
4. Divall, S.; Goodey, R.J. Twin-tunnelling-induced ground movements in clay. *Proc. Inst. Civ. Eng.-Geotech. Eng.* **2015**, *168*, 247–256. https://doi.org/10.1680/geng.14.00054.
5. Islam, M.S.; Iskander, M. Twin tunnelling induced ground settlements: A review. *Tunn. Undergr. Space Technol.* **2021**, *110*, 103614. https://doi.org/10.1016/j.tust.2020.103614.
6. Burland, J.B.; Standing, J.R.; Jardine, F.M. Assessing the risk of damage due to tunneling—Lessons from the Jubilee Line Extension, London. In Proceedings of the 14th South-East Asian Conference on Geotechnical Engineering, Hong Kong, 10–14 December 2001; pp. 17–44.
7. Mair, R.J.; Taylor, R.N. Bored tunnelling in the urban environment. In Proceedings of the 14th International Conference on Soil Mechanics and Foundation Engineering, State-of-the-art Report and Theme Lecture, Hamburg, Germany, 6–12 September 1997; pp. 2353–2385.

8. Niu, G.; He, X.; Xu, H.; Dai, S. Tunnelling-induced ground surface settlement: A comprehensive review with particular attention to artificial intelligence technologies. *Nat. Hazards Res.* **2024**, *4*, 148–168. https://doi.org/10.1016/j.nhres.2023.11.002.
9. Peck, R.B. Deep excavations and tunnelling in soft ground. In Proceedings of the 7th International Conference on Soil Mechanics and Foundations Engineering, Mexico City, Mexico, 25–29 August 1969; pp. 225–290.
10. Cording, E.J.; Hansmire, W.H. Displacement around soft ground tunnels-General report. In Proceedings of the 5th Pan-American Conference on Soil Mechanics and Foundation Engineering, Argentina, 17–22 November 1975; pp. 571–632.
11. Perez Saiz, R.; Garami, J.; Arcones, A.; Soriano, A. Experience gained through tunnel instrumentation. In Proceedings of the Tenth International Conference on Soil Mechanics and Foundation Engineering, Stockholm, Sweden, 15–19 June 1981.
12. Fargnoli, V.; Boldini, D.; Amorosi, A. Twin tunnel excavation in coarse grained soils: Observations and numerical back-predictions under free field conditions and in presence of a surface structure. *Tunn. Undergr. Space Technol.* **2015**, *49*, 454–469. https://doi.org/10.1016/j.tust.2015.06.003.
13. Suwansawat, S.; Einstein, H.H. Describing Settlement Troughs over Twin Tunnels Using a Superposition Technique. *J. Geotech. Geoenvironmental Eng.* **2007**, *133*, 445–468. https://doi.org/10.1061/(asce)1090-0241(2007)133:4(445).
14. Ghaboussi, J.; Ranken, R.E. Interaction between two parallel tunnels. *Int. J. Numer. Anal. Methods Geomech.* **1977**, *1*, 75–103.
15. Soliman, E.; Duddeck, H.; Ahrens, H. Two- and three-dimensional analysis of closely spaced double-tube tunnels. *Tunn. Undergr. Space Technol.* **1993**, *8*, 13–18. https://doi.org/10.1016/0886-7798(93)90130-n.
16. Addenbrooke, T.I.; Potts, D.M. Twin Tunnel Interaction: Surface and Subsurface Effects. *Int. J. Geomech.* **2001**, *1*, 249–271. https://doi.org/10.1061/(asce)1532-3641(2001)1:2(249).
17. Ng, C.W.; Lee, K.M.; Tang, D.K. Three-dimensional numerical investigations of new Austrian tunnelling method (NATM) twin tunnel interactions. *Can. Geotech. J.* **2004**, *41*, 523–539. https://doi.org/10.1139/t04-008.
18. Do, N.-A.; Dias, D.; Oreste, P.; Djeran-Maigre, I. Three-dimensional numerical simulation of a mechanized twin tunnels in soft ground. *Tunn. Undergr. Space Technol.* **2014**, *42*, 40–51. https://doi.org/10.1016/j.tust.2014.02.001.
19. Do, N.A.; Dias, D.; Oreste, P.; Djeran-Maigre, I. 2D numerical investigations of twin tunnel interaction. *Geomech. Eng.* **2014**, *6*, 263–275. https://doi.org/10.12989/gae.2014.6.3.263.
20. Liu, H.Y.; Small, J.C.; Carter, J.P. Full 3D modelling for effects of tunnelling on existing support systems in the Sydney region. *Tunn. Undergr. Space Technol.* **2008**, *23*, 399–420. https://doi.org/10.1016/j.tust.2007.06.009.
21. Nematollahi, M.; Dias, D. Three-dimensional numerical simulation of pile-twin tunnels interaction—Case of the Shiraz subway line. *Tunn. Undergr. Space Technol.* **2019**, *86*, 75–88. https://doi.org/10.1016/j.tust.2018.12.002.
22. Chapman, D.N.; Rogers, C.D.F.; Hunt, D.V.L. Predicting the Settlements above Twin Tunnels Constructed in Soft Ground. In Proceedings of the 30th ITA-AITES World Tunnel Congess, Sydney, Australia, 2–6 March 2002; p. 8.
23. Pedro, A.M.G.; Cancela, T.; Almeida e Sousa, J.; Grazina, J. Deformations caused by the excavation of twin tunnels. In Proceedings of the 9th International Symposium on Geotechnical Aspects of Underground Construction in Soft Ground, Sao Paulo, Brazil, 4–6 April 2017; pp. 203–213.
24. Miliziano, S.; Caponi, S.; Carlaccini, D.; de Lillis, A. Prediction of tunnelling-induced effects on a historic building in Rome. *Tunn. Undergr. Space Technol.* **2022**, *119*, 104212. https://doi.org/10.1016/j.tust.2021.104212.
25. Chapman, D.N.; Ahn, S.K.; Hunt, D.V. Investigating ground movements caused by the construction of multiple tunnels in soft ground using laboratory model tests. *Can. Geotech. J.* **2007**, *44*, 631–643. https://doi.org/10.1139/t07-018.
26. Divall, S.; Goodey, R.J.; Taylor, R.N. Ground movements generated by sequential twin-tunnelling in over-consolidated clay. In Proceedings of the 2nd European Conference on Physical Modelling in Geotechnics, Delft, The Netherlands, 23–24 April 2012; p. 10.
27. He, C.; Feng, K.; Fang, Y.; Jiang, Y.-C. Surface settlement caused by twin-parallel shield tunnelling in sandy cobble strata. *J. Zhejiang Univ. SCIENCE A* **2012**, *13*, 858–869.
28. Zheng, G.; Tong, J.; Zhang, T.; Wang, R.; Fan, Q.; Sun, J.; Diao, Y. Experimental study on surface settlements induced by sequential excavation of two parallel tunnels in drained granular soil. *Tunn. Undergr. Space Technol.* **2020**, *98*, 103347. https://doi.org/10.1016/j.tust.2020.103347.
29. Vlachopoulos, N.; Vazaios, I.; Madjdabadi, B.M. Investigation into the influence of excavation of twin-bored tunnels within weak rock masses adjacent to slopes. *Can. Geotech. J.* **2018**, *55*, 1533–1551. https://doi.org/10.1139/cgj-2017-0392.
30. Pedro, A.; Grazina, J.; Almeida e Sousa, J. Lining forces in tunnel interaction problems. *Soils Rocks* **2022**, *45*, e2022077221. https://doi.org/10.28927/sr.2022.077221.

31. Shivaei, S.; Hataf, N.; Pirastehfar, K. 3D numerical investigation of the coupled interaction behavior between mechanized twin tunnels and groundwater—A case study: Shiraz metro line 2. *Tunn. Undergr. Space Technol.* **2020**, *103*, 103458. https://doi.org/10.1016/j.tust.2020.103458.
32. Sahoo, J.P.; Kumar, J. Required Lining Pressure for the Stability of Twin Circular Tunnels in Soils. *Int. J. Geomech.* **2018**, *18*, 04018069. https://doi.org/10.1061/(asce)gm.1943-5622.0001196.
33. Yang, F.; Zheng, X.; Zhang, J.; Yang, J. Upper bound analysis of stability of dual circular tunnels subjected to surcharge loading in cohesive-frictional soils. *Tunn. Undergr. Space Technol.* **2017**, *61*, 150–160. https://doi.org/10.1016/j.tust.2016.10.006.
34. Pedro, A.M.G.; Grazina, J.C.; Almeida e Sousa, J. Stress redistribution in the central pillar between twin tunnels. In Proceedings of the NUMGE18, Porto, Portugal, 25–27 June 2018; pp. 1309–1317.
35. Zhang, T.; Taylor, R.N.; Divall, S.; Zheng, G.; Sun, J.; Stallebrass, S.E.; Goodey, R.J. Explanation for twin tunnelling-induced surface settlements by changes in soil stiffness on account of stress history. *Tunn. Undergr. Space Technol.* **2019**, *85*, 160–169. https://doi.org/10.1016/j.tust.2018.12.015.
36. O'Reilly, M.P.; New, B.M. Settlements above tunnel in the United Kingdom—Their magnitude and prediction. In Proceedings of the Conference Tunnelling '82, London, UK, 7–11 June 1982; pp. 173 -181.
37. Ocak, I. A new approach for estimating the transverse surface settlement curve for twin tunnels in shallow and soft soils. *Environ. Earth Sci.* **2014**, *72*, 2357–2367. https://doi.org/10.1007/s12665-014-3145-5.
38. Zhou, Z.; Ding, H.; Miao, L.; Gong, C. Predictive model for the surface settlement caused by the excavation of twin tunnels. *Tunn. Undergr. Space Technol.* **2021**, *114*, 104014. https://doi.org/10.1016/j.tust.2021.104014.
39. Hunt, D.V.L. Predicting the ground movements above twin tunnels constructed in London Clay. Ph.D. Thesis, University of Birmingham, Birmingham, UK, 2005.
40. Dong, C.; Lin, J.; Cao, G.; Cheng, H.; Shi, L.; Zhang, X. Analytical Study on Surface Settlement Troughs Induced by the Sequential Excavation of Adjacent and Parallel Tunnels in Layered Soils. *Adv. Civ. Eng.* **2022**, *2022*, 2489711. https://doi.org/10.1155/2022/2489711.
41. Ou, C.-Y.; Hwang, R.N.; Lai, W.-J. Surface settlement during shield tunnelling at CH218 in Taipei. *Can. Geotech. J.* **1998**, *35*, 159–168.
42. Withers, A.D. Chapter 37—Surface displacements at three surface reference sites above twin tunnels through the Lambeth Group. In *Building Response to Tunnelling*; Thomas Telford Publishing: London, UK, 2001; pp. 735–754.
43. Wu, B.R.; Lee, C.J. Ground movements and collapse mechanisms induced by tunneling in clayey soil. *Int. J. Phys. Model. Geotech.* **2003**, *3*, 15–29. https://doi.org/10.1680/ijpmg.2003.030402.
44. Clayton, C.; Van Der Berg, J.; Thomas, A. Monitoring and displacements at Heathrow Express Terminal 4 station tunnels. *Géotechnique* **2006**, *56*, 323–334.
45. Mahmutoğlu, Y. Surface subsidence induced by twin subway tunnelling in soft ground conditions in Istanbul. *Bull. Eng. Geol. Environ.* **2011**, *70*, 115–131. https://doi.org/10.1007/s10064-010-0289-8.
46. Bilotta, E.; Russo, G. Ground movements induced by tunnel boring in Naples. In Proceedings of the 7th International Symposium on Geotechnical Aspects of Underground Construction in Soft Ground, Roma, Italy, 17–19 May 2011.
47. Standing, J.R.; Selemetas, D. Greenfield ground response to EPBM tunnelling in London Clay. *Géotechnique* **2013**, *63*, 989–1007. https://doi.org/10.1680/geot.12.P.154.
48. Elwood, D.E.Y.; Martin, C.D. Ground response of closely spaced twin tunnels constructed in heavily overconsolidated soils. *Tunn. Undergr. Space Technol.* **2016**, *51*, 226–237. https://doi.org/10.1016/j.tust.2015.10.037.
49. Wan, M.S.P.; Standing, J.R.; Potts, D.M.; Burland, J.B. Measured short-term ground surface response to EPBM tunnelling in London Clay. *Géotechnique* **2017**, *67*, 420–445. https://doi.org/10.1680/jgeot.16.P.099.
50. Zhong, Z.; Li, C.; Liu, X.; Fan, Y.; Liang, N. Analysis of ground surface settlement induced by the construction of mechanized twin tunnels in soil-rock mass mixed ground. *Tunn. Undergr. Space Technol.* **2021**, *110*, 103746. https://doi.org/10.1016/j.tust.2020.103746.
51. Kannangara, K.K.P.M.; Ding, Z.; Zhou, W.-H. Surface settlements induced by twin tunneling in silty sand. *Undergr. Space* **2022**, *7*, 58–75. https://doi.org/10.1016/j.undsp.2021.05.002.
52. Hu, Y.; Tang, H.; Xu, Y.; Lei, H.; Zeng, P.; Yao, K.; Dong, Y. Ground settlement and tunnel response due to twin-curved shield tunnelling in soft ground with small clear distance. *J. Rock Mech. Geotech. Eng.* **2024**, *16*, 3122–3135. https://doi.org/10.1016/j.jrmge.2024.06.005.

53. Mooney, M.; Grasmick, J.; Clemmensen, A.; Thompson, A.; Prantil, E.; Robinson, B. Ground deformation from multiple tunnel openings: Analysis of Queens Bored Tunnels. In Proceedings of the North American Tunneling, Los Angeles, CA, USA, 22–25 June 2014.
54. Pedro, A.M.G.; Grazina, J.C.D.; Sousa, J.A.e. Influence of the pillar width on the construction sequence of twin tunnels. In Proceedings of the NUMGE23—10th European Conference on Numerical Methods in Geotechnical Engineering, London, UK, 2023.
55. Divall, S. Ground movements associated with twin-tunnel construction in clay. PhD thesis, City University London, London, UK, 2013.
56. Divall, S.; Goodey, R.J.; Stallebrass, S.E. Twin-tunnelling-induced changes to clay stiffness. *Géotechnique* **2017**, *67*, 906–913. https://doi.org/10.1680/jgeot.sip17.P.151.
57. Chen, S.L.; Gui, M.W.; Yang, M.C. Applicability of the principle of superposition in estimating ground surface settlement of twin- and quadruple-tube tunnels. *Tunn. Undergr. Space Technol.* **2012**, *28*, 135–149.